Gravitational Form Factors and Mechanical Properties of the Proton

ASMITA MUKHERJEE

Indian Institute of Technology Bombay

In collaboration with D. Chakrabarti, C. Mondal, S. Nair, X. Zhao

PRD 102, 113011 (2020)

QCD Evolution workshop, May 10-14, 2021

Gravitational Form Factors (GFFs)

$$\langle P', S'|T_i^{\mu\nu}(0)|P, S\rangle = \bar{U}(P', S')\Big[-B_i(q^2)\frac{\bar{P}^\mu \bar{P}^\nu}{M} + (A_i(q^2) + B_i(q^2))\frac{1}{2}(\gamma^\mu \bar{P}^\nu + \gamma^\nu \bar{P}^\mu)$$
$$+ C_i(q^2)\frac{q^\mu q^\nu - q^2 g^{\mu\nu}}{M} + \bar{C}_i(q^2) M g^{\mu\nu}\Big] U(P, S),$$

$\bar{P}^\mu = \frac{1}{2}(P' + P)^\mu$, $q^\mu = (P' - P)^\mu$

We choose Drell-Yan frame $Q^2 = -q^2 = \vec{q}_\perp^{\,2}$

GFFs give how matter couples to gravity

$$P = (P^+, P_\perp, P^-) = \left(P^+, 0, \frac{M^2}{P^+}\right),$$

$$P' = (P'^+, P'_\perp, P'^-) = \left(P^+, q_\perp, \frac{q_\perp^2 + M^2}{P^+}\right)$$

$$q = P' - P = \left(0, q_\perp, \frac{q_\perp^2}{P^+}\right),$$

GFFS

$A(Q^2)$ and $B(Q^2)$ are related to the mass and angular momentum of the proton

$$\int dx x[H_q(x,0,0) + E_q(x,0,0)] = A_q(0) + B_q(0) = 2J_q$$

X. Ji, PRD, 1997

H_q and E_q are generalized parton distributions (GPDs) that can be accessed in exclusive processes like DVCS or deeply virtual meson production

Poincare invariance imposes the constraint :

$$\sum_{a=q,g} A_a(0) = 1, \quad \sum_{a=q,g} B_a(0) = 0, \quad \sum_{a=q,g} \bar{C}_a(t) = 0.$$

Total gravitomagnetic moment is zero follows from the equivalence principle of GTR

$\bar{C}(Q^2)$ arises due to non-conservation of EM tensor separately for quarks and gluons, and must vanish when summed over both

Lorce, Moutarde, Trawinski, EPJC (2019)

GFFs and Pressure Distribution

However, $C(Q^2)$, also called the D-term, is not related to any Poincare generator and is unconstrained

D term is related to the pressure and shear force distribution inside the nucleon

Polyakov and Schweitzer, IJMPA (2018)

Recent result from Jlab showed that the pressure distribution at the center of the nucleon is repulsive and confining towards the outer region

Burkert, Elouadrhiri, Girod, Nature(2018)

This also connects a set of collider observables (GPDs) to the investigation of the equation of state (EoS) of neutron stars

Rajan, Gorda, Liuti, Yagi (2018)

Quite a lot of theoretical calculations in recent days

Pressure distribution inside the nucleon

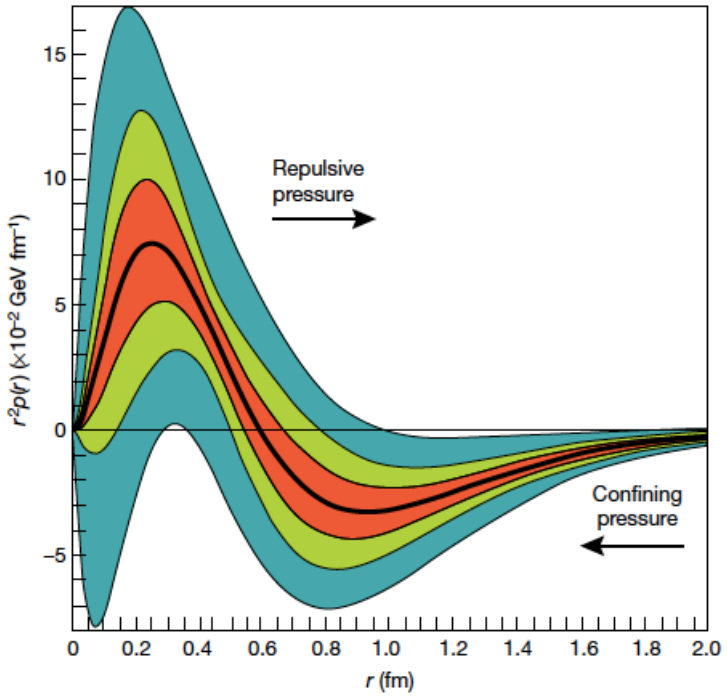

Pressure distribution obtained from fits to Jlab data to extract the GPDs, in particular the D-term

Pressure distribution is repulsive at the center of the nucleon and confining in the outer region

At the core it exceeds the pressure density of the most dense object that is neutron star , average peak pressure 10^{35} Pascals

Burkert, Elouadrhiri, Girod, Nature(2018)

GFFs and Pressure Distribution

Jlab result triggered a lot of interest : theoretical model calculations of the pressure distributions

Polyakov and Schweitzer, IJMPA (2018)

Most calculations are done in the Breit frame and are subject to relativistic corrections

2-D distributions in the infinite momentum frame or light-front formalism introduced in

Lorce, Moutarde, Trawinski, EPJC (2019)

Because of transverse Galilean symmetry on the light-front these are free from relativistic corrections

Connection between 2D and 3D pressure distributions can be established through Abel transformation

Panteleeva and Polyakov, 2021

Model calculation of GFFs

Light-front quark diquark model, where the two-particle LFWFs are modelled from the solution of soft-wall Ads/QCD

Chakrabarti, Mondal (2013)

Included only scalar diquarks in this work

$$|P;\uparrow(\downarrow)\rangle = \sum_q \int \frac{dx\, d^2\mathbf{k}_\perp}{2(2\pi)^3\sqrt{x(1-x)}} \left[\psi^{\uparrow(\downarrow)}_{+q}(x,\mathbf{k}_\perp)|+\frac{1}{2},0;xP^+,\mathbf{k}_\perp\rangle + \psi^{\uparrow(\downarrow)}_{-q}(x,\mathbf{k}_\perp)|-\frac{1}{2},0;xP^+,\mathbf{k}_\perp\rangle\right].$$

$$\begin{aligned}
\psi^{\uparrow}_{+q}(x,\mathbf{k}_\perp) &= \varphi^{(1)}_q(x,\mathbf{k}_\perp)\,,\\
\psi^{\uparrow}_{-q}(x,\mathbf{k}_\perp) &= -\frac{k^1+ik^2}{xM}\,\varphi^{(2)}_q(x,\mathbf{k}_\perp)\,,\\
\psi^{\downarrow}_{+q}(x,\mathbf{k}_\perp) &= \frac{k^1-ik^2}{xM}\,\varphi^{(2)}_q(x,\mathbf{k}_\perp)\,.\\
\psi^{\downarrow}_{-q}(x,\mathbf{k}_\perp) &= \varphi^{(1)}_q(x,\mathbf{k}_\perp),
\end{aligned}$$

$$\varphi^{(i)}_q(x,\mathbf{k}_\perp) = N^{(i)}_q \frac{4\pi}{\kappa}\sqrt{\frac{\log(1/x)}{1-x}}\, x^{a^{(i)}_q}(1-x)^{b^{(i)}_q} \exp\left[-\frac{\mathbf{k}^2_\perp}{2\kappa^2}\frac{\log(1/x)}{(1-x)^2}\right].$$

Ads/QCD scale parameter $\kappa = 0.4$ GeV

Parameters are obtained from fits of electromagnetic form factors

Model Calculations of GFFs

$$A^q(Q^2) = \mathcal{I}_1^q(Q^2),$$
$$B^q(Q^2) = \mathcal{I}_2^q(Q^2),$$
$$C^q(Q^2) = -\frac{1}{4Q^2}\left[2M^2\mathcal{I}_1^q(Q^2) - Q^2\mathcal{I}_2^q(Q^2) - \mathcal{I}_3^q(Q^2)\right],$$
$$\bar{C}^q(Q^2) = -\frac{1}{4M^2}\left[\mathcal{I}_3^q(Q^2) - \mathcal{I}_4^q(Q^2)\right],$$

C(Q^2) diverges as Q^2=0 ; artifact of the LFWFs

To avoid this we fit C(Q^2) in the region Q^2>0.1 GeV^2 and analytically continue to low Q^2

$$\mathcal{I}_1^q(Q^2) = \int dx x\left[{N_1}^2 x^{2a_1}(1-x)^{2b_1+1} + {N_2}^2 x^{2a_2-2}(1-x)^{2b_2+3}\frac{1}{M^2}\left(\frac{\kappa^2}{\log(1/x)} - \frac{Q^2}{4}\right)\right]\exp\left[-\frac{\log(1/x)}{\kappa^2}\frac{Q^2}{4}\right],$$
$$\mathcal{I}_2^q(Q^2) = 2\int dx\ N_1 N_2 x^{a_1+a_2}(1-x)^{b_1+b_2+2}\exp\left[-\frac{\log(1/x)}{\kappa^2}\frac{Q^2}{4}\right],$$
$$\mathcal{I}_3^q(Q^2) = 2\int dx N_2 N_1 x^{a_1+a_2-2}(1-x)^{b_1+b_2+2}$$
$$\times\left[\frac{4(1-x)^2\kappa^2}{\log(1/x)} + Q^2(1-x)^2 - 4m^2\right]\exp\left[-\frac{\log(1/x)}{\kappa^2}\frac{Q^2}{4}\right],$$
$$\mathcal{I}_4^q(Q^2) = -2\int dx\ N_2 N_1 x^{a_1+a_2-2}(1-x)^{b_1+b_2+2}\left[\frac{\kappa^2(1-x)^2}{\log(1/x)} + \frac{Q^2(1-x)^2}{4} + m^2\right]\exp\left[-\frac{\log(1/x)}{\kappa^2}\frac{Q^2}{4}\right].$$

GFF $C(Q^2)$

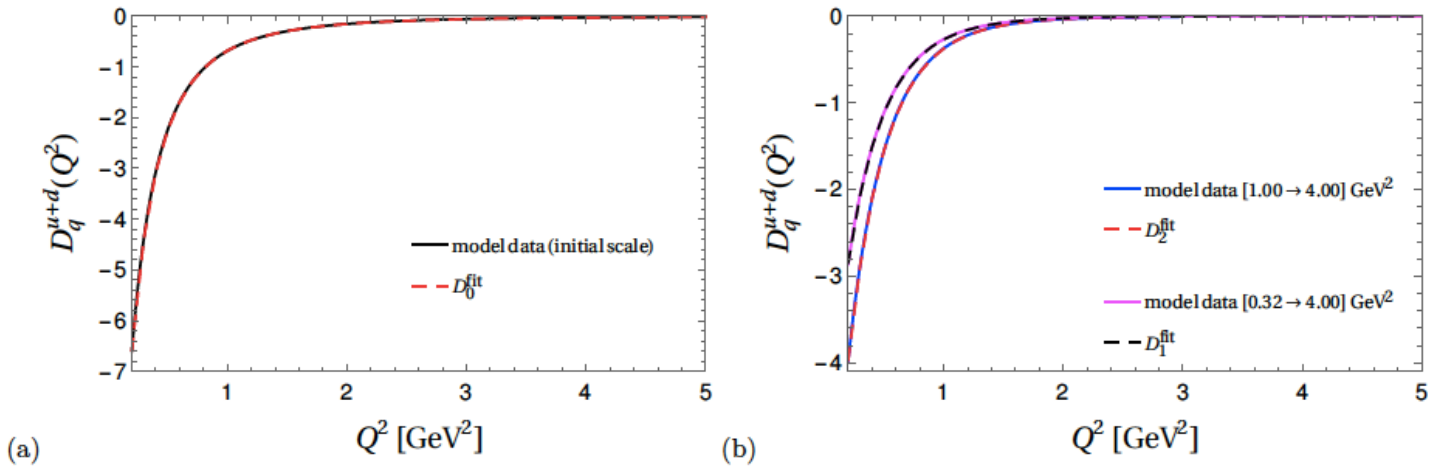

$C(Q^2)$ diverges as $Q^2=0$; artifact of the LFWFs

To avoid this we fit $C(Q^2)$ in the region $Q^2>0.1$ GeV^2 and analytically continue to low Q^2

Multipole function used for the fit

$$D^q_{\text{fit}}(Q^2) = 4C^q_{\text{fit}}(Q^2) = \frac{a_q}{(1+b_q Q^2)^{c_q}},$$

Scale evolution is encoded in the model parameters which are considered to be scale dependent, and evolved in a way that the pdfs obey the DGLAP equation; following the approach of

Maji, Mondal, Chakrabarti; PRD (2017)

Numerical results for the GFFs

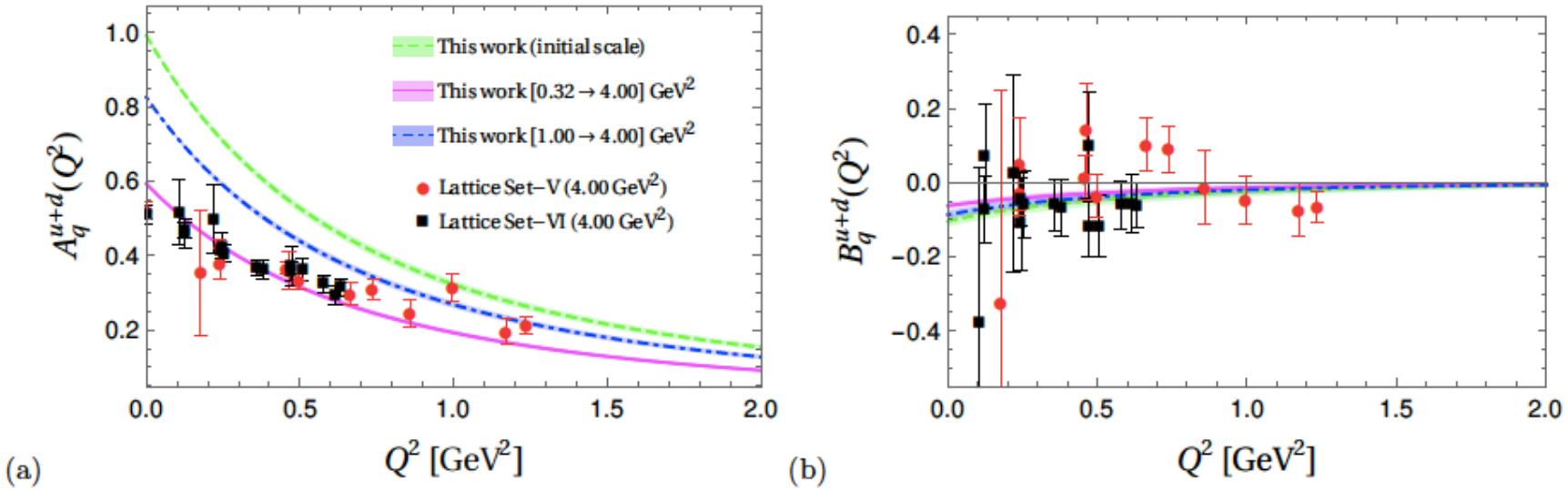

Lattice: LHPC Collaboration, PRD (2008)

To compare with lattice result we evolve our results to $\mu^2 = 4$ GeV^2 using DGLAP evolution (integrands in our model calculation are $xH_q(x, Q^2)$ and $x E_q(x, Q^2)$ respectively)

Chakrabarti, Mondal, Mukherjee, Nair, Zhao; PRD(2020)

Numerical Results

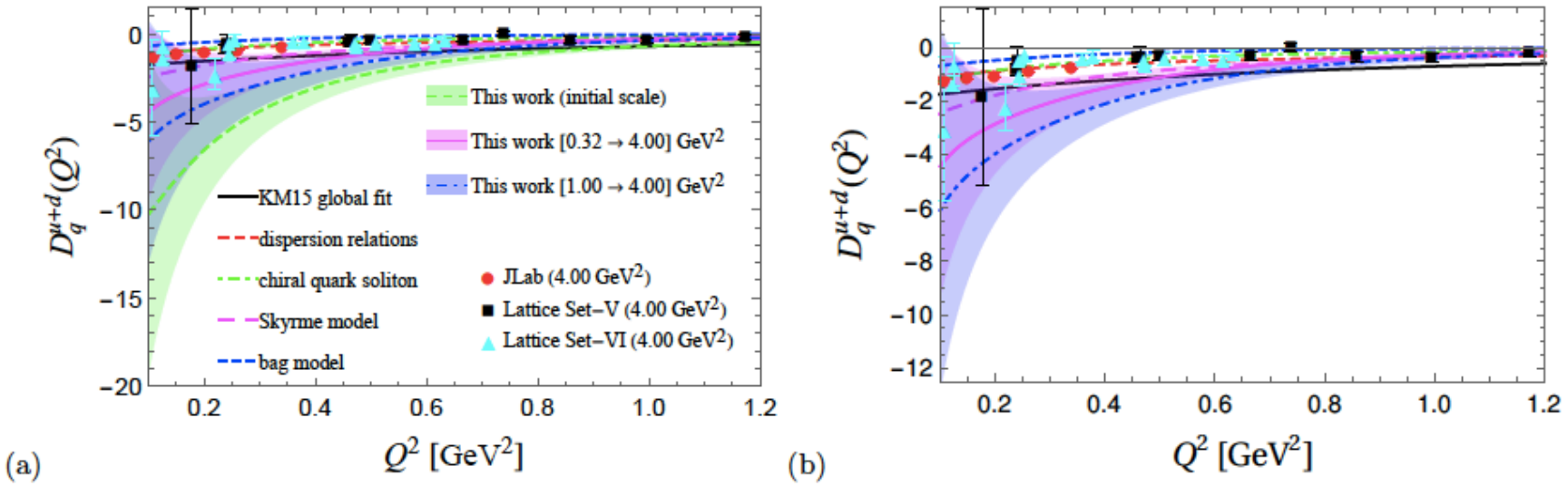

$$D_q^{u+d}(Q^2) = 4C_q^{u+d}(Q^2)$$

KM15 : Kumericki and Muller (2016)

Dispersion relation : Pasquini, Polayakov and Vanderhaeghen (2014)

Chiral Quark Soliton : K. Goeke et al (2007)

Skyrme mdel : Cebulla et al (2007)

Bag model : X. Ji et al (1997)

Uncertainty shows the FF depends strongly on model parameters

Chakrabarti, Mondal, Mukherjee, Nair, Zhao; PRD(2020)

Numerical Results

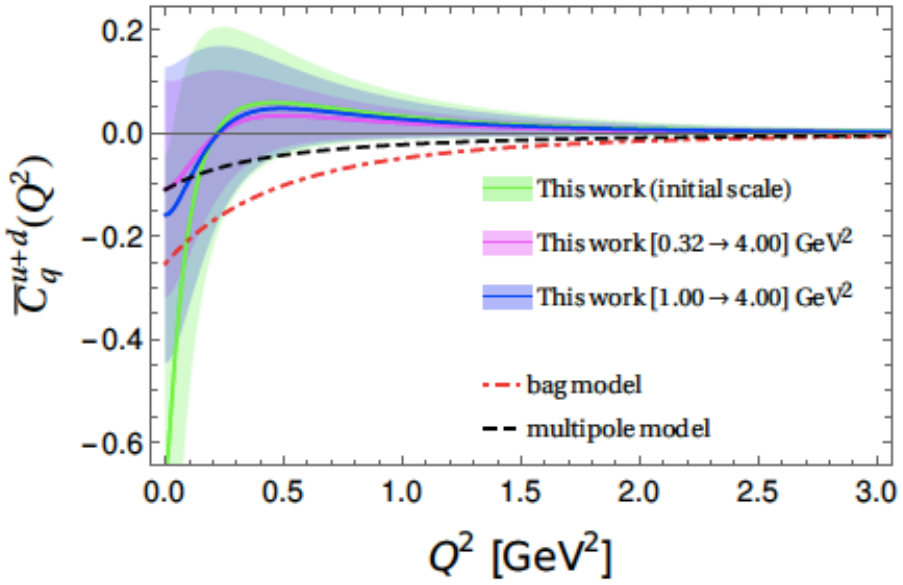

Multipole model : Lorce, Moutarde, Trawinski (2019)

Bag model : X. Ji et al (1997)

$\bar{C}(Q^2)$ Is negative for small Q^2 but positive for higher values of Q^2

In contrast with other models, where it is negative

Error bands correspond to 2% uncertainty in model parameters

Chakrabarti, Mondal, Mukherjee, Nair, Zhao; PRD(2020)

Pressure and Energy Density at the Center

Pressure and energy density at the center of the nucleon

$$p_0 = -\frac{1}{24\pi^2 M_n}\int_0^\infty \mathrm{d}Q^2\; Q^3\; D(Q^2),$$

$$\mathcal{E} = \frac{M_n}{4\pi^2}\int_0^\infty \mathrm{d}Q^2 \left(A(Q^2) + \frac{Q^2}{4M_n^2}D(Q^2)\right),$$

Mechanical radius

$$\langle r^2_{\rm mech}\rangle = 6D_{\rm fit}(0)\Big[\int_0^\infty \mathrm{d}Q^2\; D(Q^2)\Big]^{-1}.$$

TABLE III. The mechanical properties: pressure, energy density, and mechanical radius of nucleon.

Approaches/Models	p_0 [GeV/fm^3]	$\mathcal{E}$ [GeV/fm^3]	$\langle r^2_{\rm mech}\rangle$ [fm^2]
This work ($\sqrt{0.32}$ GeV $\to$ 2 GeV)	0.29	3.21	0.74
This work (1.00 GeV $\to$ 2 GeV)	0.40	4.58	0.74
QCDSR set-I (1 GeV) [8]	0.67	1.76	0.54
QCDSR set-II (1 GeV) [8]	0.62	1.74	0.52
Skyrme model [10]	0.47	2.28	-
modified Skyrme model [11]	0.26	1.445	-
χQSM [7]	0.23	1.70	-
Soliton model [9]	0.58	3.56	-
LCSM-LO [4]	0.84	0.92	0.54

Pressure and Shear Distribution

Pressure and shear force distributions are defined as

$$p(b) = \frac{1}{6M_n}\frac{1}{b^2}\frac{d}{db}b^2\frac{d}{db}\tilde{D}(b),$$

$$s(b) = -\frac{1}{4M_n}b\frac{d}{db}\frac{1}{b}\frac{d}{db}\tilde{D}(b),$$

Where $\tilde{D}(b) = \int \frac{\mathrm{d}^2\vec{q}_\perp}{(2\pi)^2}\, e^{i\vec{q}_\perp\cdot\vec{b}_\perp} D(Q^2).$

The pressure distribution has to obey the von Laue condition for stability $\int_0^\infty db\, b^2\, p(b) = 0.$

This is a consequence of the conservation of energy-momentum tensor

b represents the impact parameter

Pressure and Shear Distribution

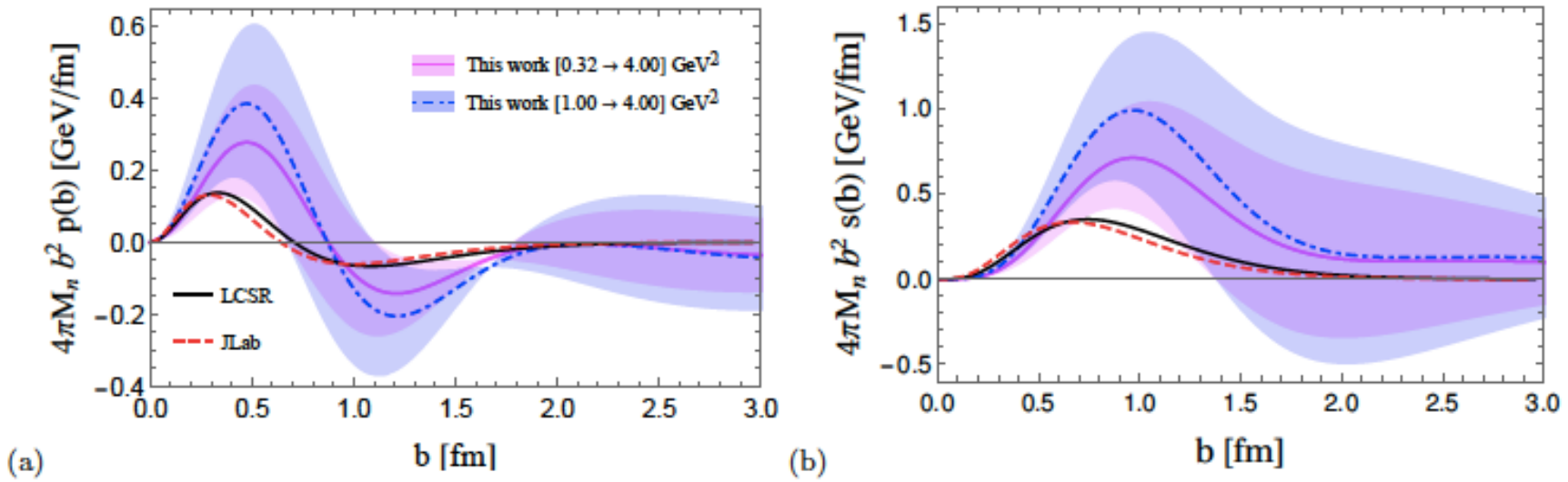

Pressure and shear distribution compared with Burkert, Elouadrhiri, Girod, Nature(2018) and
Light cone sum rule approach Anikin, PRD (2019)

Qualitative behavior similar to other calculations

Pattern ensures mechanical stability: repulsive core prevents the system from collapsing and the attractive Force away from center binds the system.

Shear distribution : related to surface tension and surface energy; which are positive in stable hydrostatic systems.

Chakrabarti, Mondal, Mukherjee, Nair, Zhao; PRD(2020)

Normal and tangential force

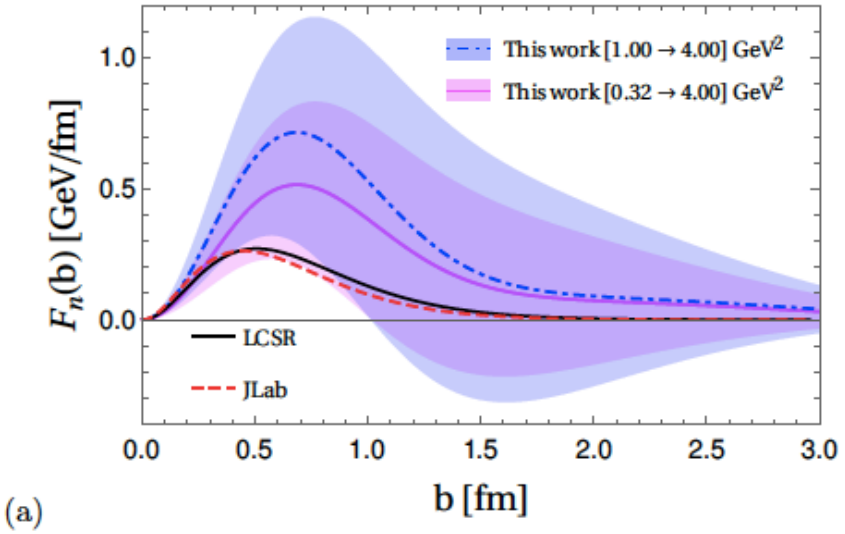

(a)

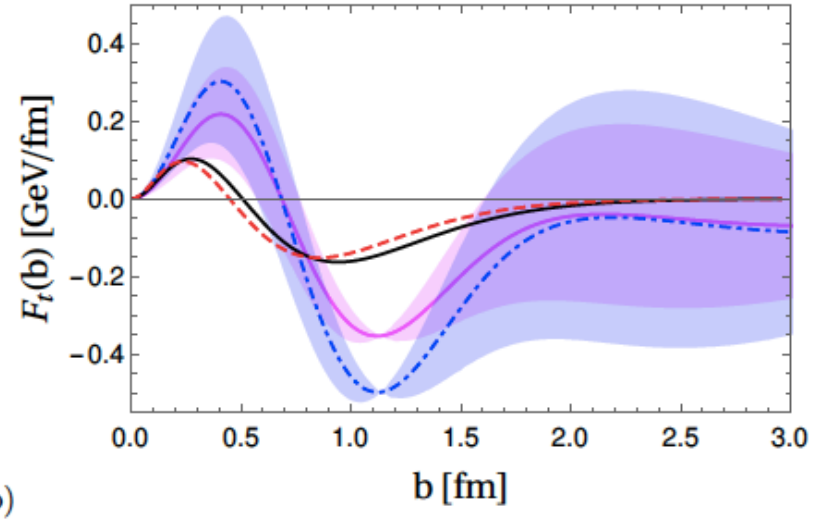

(b)

A spherical shell of radius b inside the nucleon experiences radial and tangential force

$$F_n(b) = 4\pi M_n b^2 \left(p(b) + \frac{2}{3} s(b) \right),$$

$$F_t(b) = 4\pi M_n b^2 \left(p(b) - \frac{1}{3} s(b) \right).$$

Qualitative behavior of radial and tangential force similar to light cone sum rule and fits to Jlab data

Tangential force positive near the center, negative in the outer region

Chakrabarti, Mondal, Mukherjee, Nair, Zhao; PRD(2020)

2D energy density

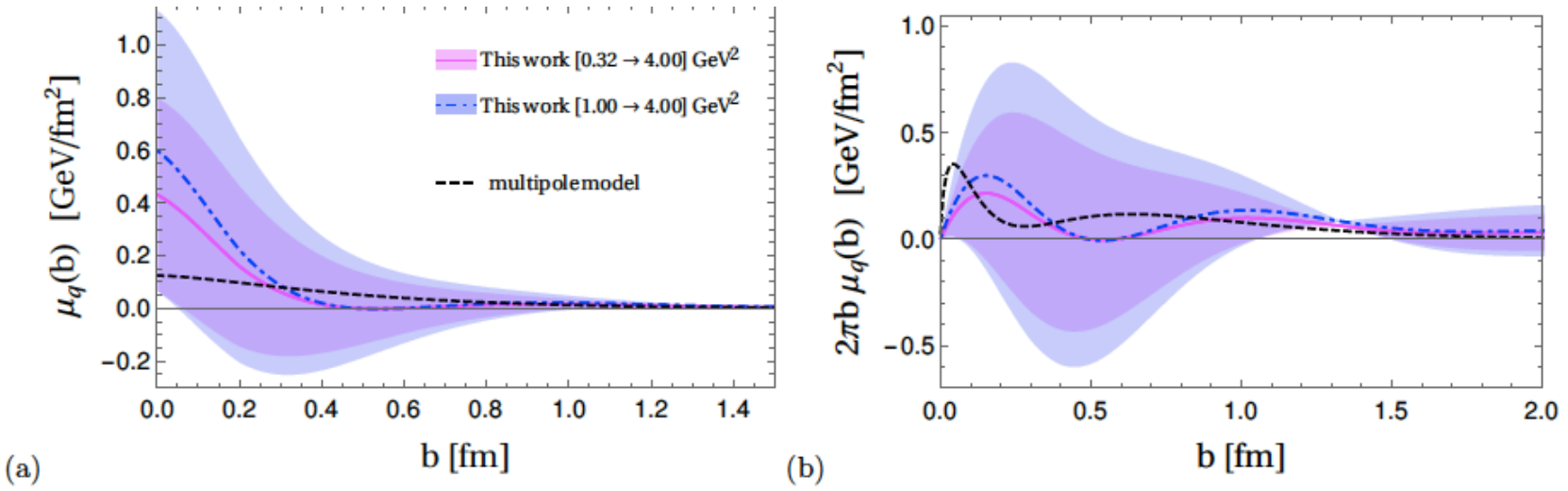

Energy density has a peak at the center, consistent with the simple multipole model of C. Lorce et al EPJC (2019)

$$\mu_a(b) = M_n\left\{\frac{A_a(b)}{2} + \bar{C}_a(b) + \frac{1}{4M_n^2}\frac{1}{b}\frac{d}{db}\left(b\frac{d}{db}\left[\frac{B_a(b)}{2} - 4C_a(b)\right)\right]\right\} \qquad \chi(b) = \int \frac{\mathrm{d}^2\vec{q}_\perp}{(2\pi)^2}\, e^{i\vec{q}_\perp.\vec{b}_\perp}\chi(q^2).$$

Chakrabarti, Mondal, Mukherjee, Nair, Zhao; PRD(2020)

2D radial pressure

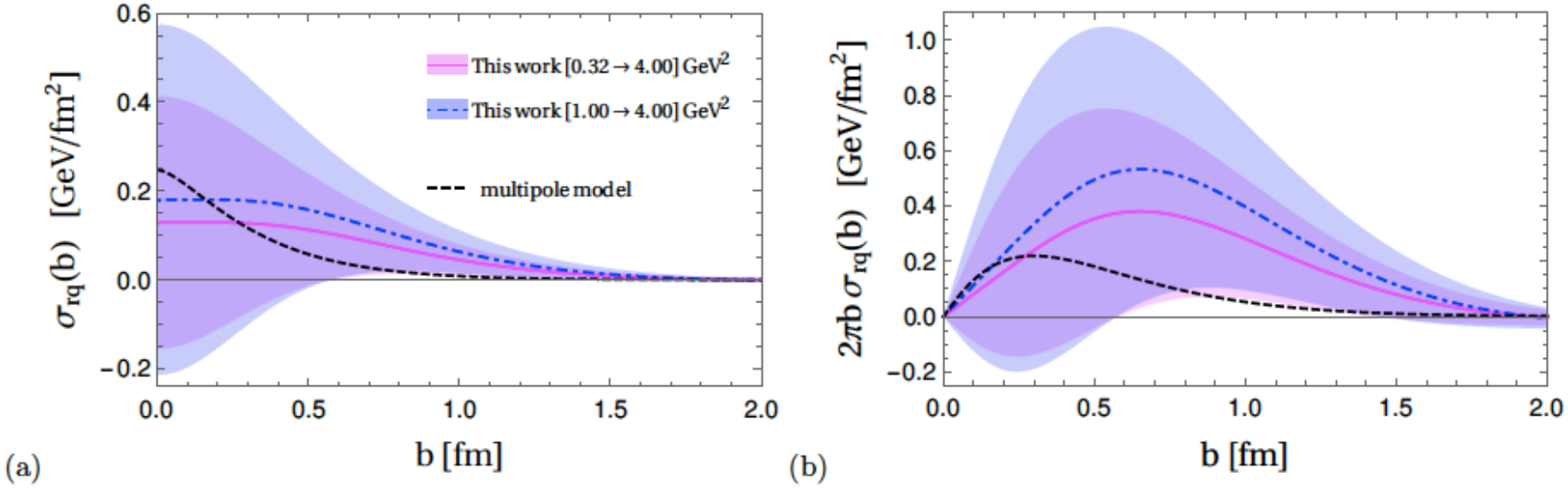

$$\sigma_{r,a}(b) = M_n\Big\{ -\bar{C}_a(b) + \frac{1}{M_n^2}\frac{1}{b}\frac{dC_a(b)}{db}\Big\}$$

$$\chi(b) = \int \frac{\mathrm{d}^2\vec{q}_\perp}{(2\pi)^2}\, e^{i\vec{q}_\perp.\vec{b}_\perp}\chi(q^2).$$

Chakrabarti, Mondal, Mukherjee, Nair, Zhao; PRD(2020)

2D tangential pressure

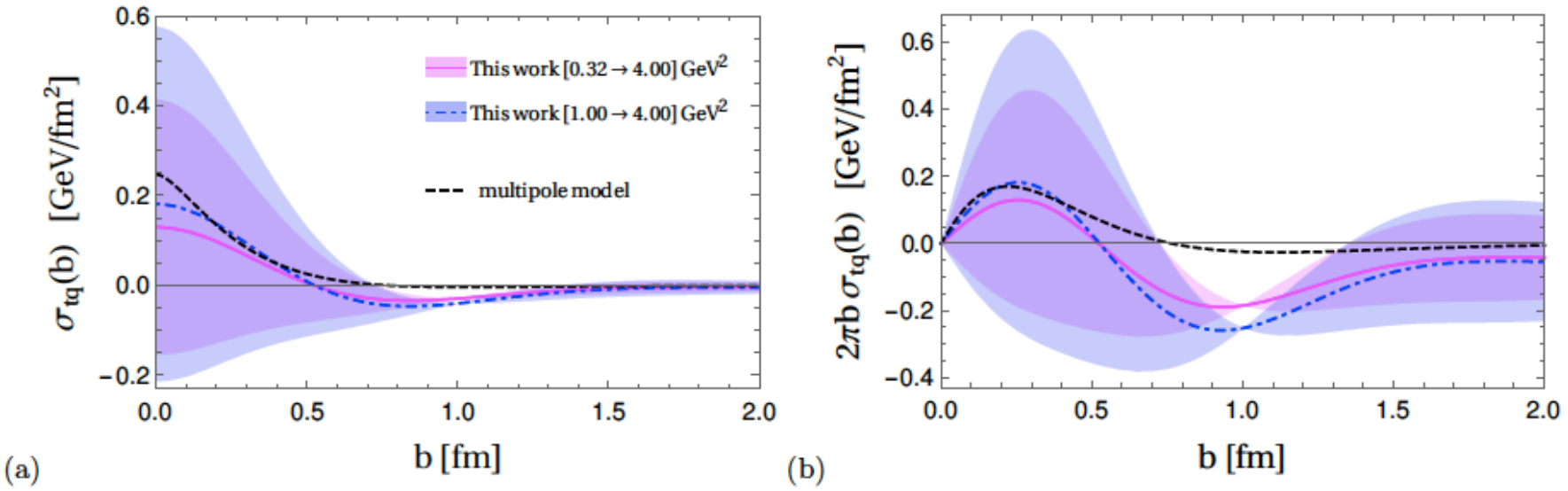

$$\sigma_{t,a}(b) = M_n \Big\{ -\bar{C}_a(b) + \frac{1}{M_n^2}\frac{d^2 C_a(b)}{db^2} \Big\}$$

$$\chi(b) = \int \frac{\mathrm{d}^2\vec{q}_\perp}{(2\pi)^2}\, e^{i\vec{q}_\perp.\vec{b}_\perp}\chi(q^2).$$

Chakrabarti, Mondal, Mukherjee, Nair, Zhao; PRD(2020)

2D Isotropic pressure

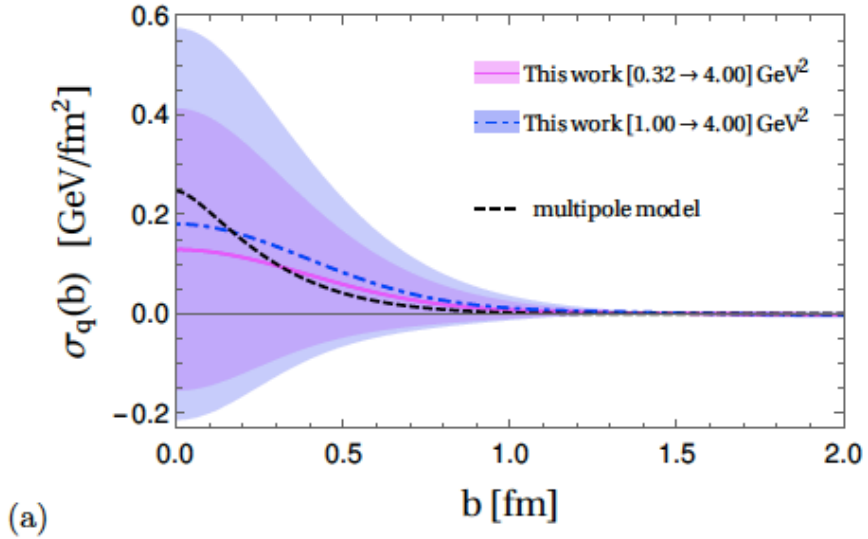

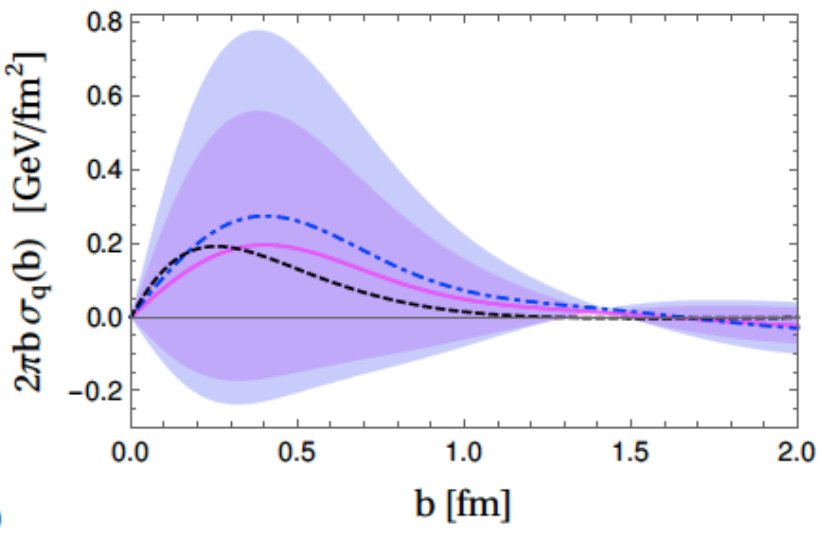

$$\sigma_a(r) = \frac{\sigma_{ra}(r) + 2\sigma_{ta}(r)}{3}$$

$$\sigma_a(b) = M_n \Big\{ -\bar{C}_a(b) + \frac{1}{2}\frac{1}{M_n^2}\frac{1}{b}\frac{d}{db}\left(b\frac{dC_a(b)}{db}\right) \Big\}$$

$$\chi(b) = \int \frac{\mathrm{d}^2\vec{q}_\perp}{(2\pi)^2}\, e^{i\vec{q}_\perp.\vec{b}_\perp}\chi(q^2).$$

Chakrabarti, Mondal, Mukherjee, Nair, Zhao; PRD(2020)

2D Pressure Anisotropy

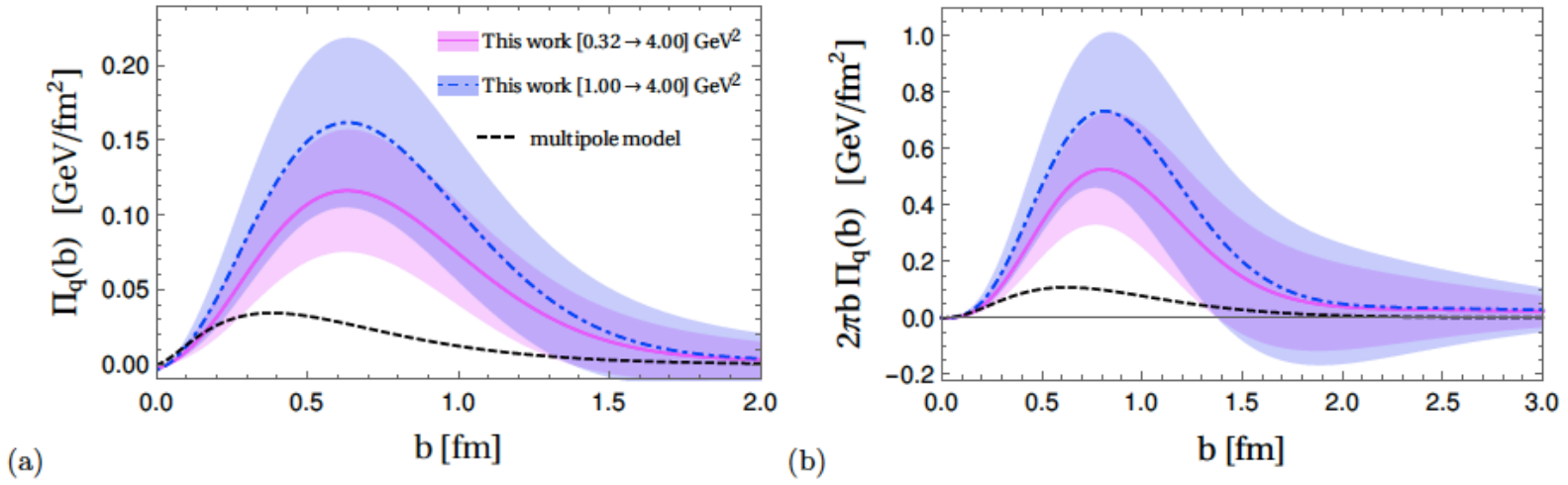

Vanishes at center due to spherical symmetry

Positive away from center : radial pressure larger than tangential pressure

$$\Pi_a(r) = \sigma_{ra}(r) - \sigma_{ta}(r)$$

$$\Pi_a(b) = M_n\Big\{ -\frac{1}{M_n^2} b\frac{d}{db}\left(b\frac{dC_a(b)}{db}\right)\Big\}$$

$$\chi(b) = \int \frac{\mathrm{d}^2\vec{q}_\perp}{(2\pi)^2}\, e^{i\vec{q}_\perp.\vec{b}_\perp}\chi(q^2).$$

Chakrabarti, Mondal, Mukherjee, Nair, Zhao; PRD(2020)

Conclusion

We presented a calculation of the GFF and pressure distributions in the proton using a light-front quark-diquark model with Ads/QCD predicted wave functions

$A(Q^2)$ and $B(Q^2)$ in this model are comparable with lattice result

Qualitative behaviour of $D(Q^2)$ agrees with other model calculations. $D(Q^2)$ is negative and the magnitude at $Q^2=0$ is larger than obtained in other models. $D(Q^2)$ can be described by a multipole form.

$\bar{C}(Q^2)$ Is negative for lower values of Q^2 but positive for higher values; in contrast with other model calculations

Presented the pressure and energy distributions and mechanical radius : compared with other calculations

Qualitative behavior of the pressure and shear distributions agree with other model calculations as well as that observed from Jlab data